

Phase equilibria in binary Lennard-Jones mixtures: phase diagram simulation

J. N. CANONGIA LOPES

Centro de Química Estrutural, Instituto Superior Técnico, 1096 Lisboa, Portugal

(Received 23 October 1998; accepted 12 January 1999)

A three-box version of the Gibbs ensemble Monte Carlo method was used to determine the phase diagram type of several binary mixtures of one-centre Lennard-Jones particles. The method can be used to establish a direct link between the intermolecular potential modelling the interactions in a given system and its fluid phase diagram, without the knowledge of the corresponding equation of state governing its pVT behaviour. As an example of the application of the method, closed-loop behaviour in an isotropic system could be found using a set of Lennard-Jones parameters exhibiting a cross-interaction diameter with a negative deviation from the Lorentz–Berthelot combination rule.

1. Introduction

The prediction of thermodynamic properties based on the modelling of molecular interactions is a central aspect of equilibrium statistical mechanics. Computer simulation is one of the tools presently available to implement such type of calculation.

Since its introduction in 1987 [1], the Gibbs ensemble Monte Carlo (GEMC) method has proved to be one of the most effective ways to simulate two coexisting phases in equilibrium. The method has been applied successfully to the study of liquid–vapour (LV), liquid–liquid (LL) and osmotic equilibria in a wide range of fluids and fluid mixtures [2].

In the GEMC method, the coexisting phases are simulated in two separate subsystems (the Gibbs ensemble), avoiding the direct simulation of the interface between the two bulk phases. Equilibrium is reached by allowing three types of Monte Carlo moves within and between the subsystems: particle displacements inside each simulation box, volume exchange between boxes (the total volume is kept constant) and particle transfer from one box to another (the total number of particles and composition are kept constant). While the first type of move is responsible for the attainment of internal equilibrium in each subsystem, the last two ensure the pressure and chemical potential balances throughout the system.

In a recent paper [3] the method was extended to the study of more than two phases in equilibrium, allowing the simulation to occur in a number of simulation boxes matching the number of coexisting phases. Several test systems were analysed where liquid–liquid immiscibility leads to three-phase equilibria in binary and ternary mixtures (liquid–liquid–vapour equilibria) and four

phase equilibria in ternary mixtures (systems with triple liquid immiscibility).

The occurrence of liquid–liquid immiscibility in binary mixtures and its relation to the liquid–vapour critical phenomena define several types of phase behaviour into which binary mixtures can be classified. The phase diagrams corresponding to most of these types exhibit three-phase lines delimited by lower and/or upper critical solution temperature end points (LCEP and UCEP) and can be studied using the three-box version of the GEMC method.

2. Binary mixture types

In the present work binary mixtures will be analysed according to the classification proposed by Scott and van Konynenburg [4]. These authors showed that the van der Waals equation can account qualitatively for almost all kinds of fluid phase behaviour encountered experimentally and defined six types of binary mixture divided into three classes. Some types comprise several subtypes but these will not be discussed here.

Although theirs is not the only possible classification—for instance type VI was not included in their original discussion due to the impossibility of its prediction within the framework of the van der Waals 1-fluid approximation, and type VII has been subsequently introduced [5] to define a ‘hybrid’ type between types V and VI—their systematic work establishing the boundaries for each type of mixture remains a reference.

The six types of binary mixture can be best understood considering their (p, T) projections (figure 1). Basically, types I and II form Class 1, i.e. mixtures of two components with similar gas–liquid critical tem-

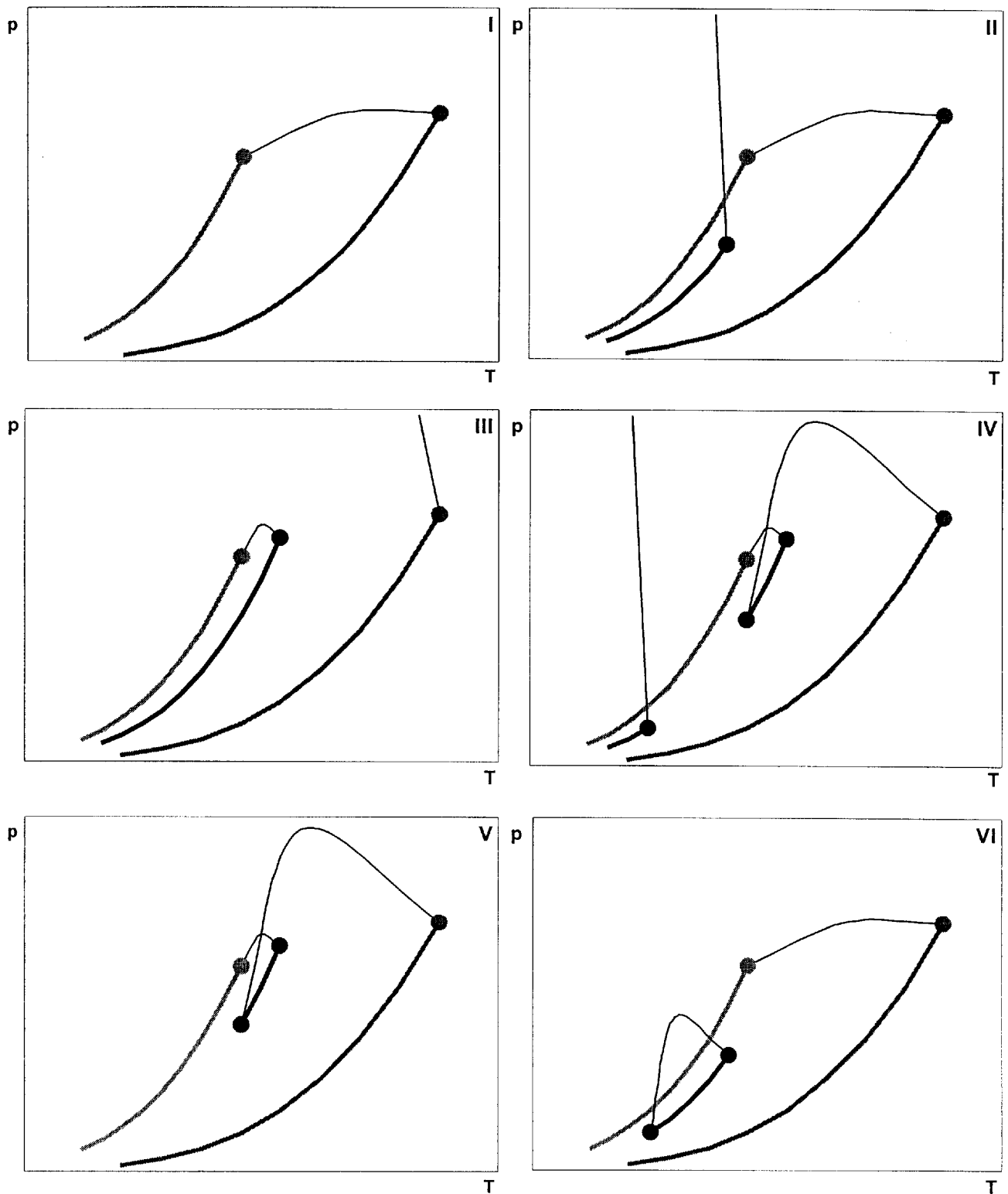


Figure 1. The p - T projections for the six types of binary phase diagram [4]. The grey lines represent the saturation curves of the two pure components, the black thick lines the three-phase line (liquid-liquid-vapour equilibria) of the mixtures and the thin lines the end of the two-phase surfaces (liquid-liquid and liquid-vapour critical lines). The points marking the end of each thick line (critical points of the pure components and upper and lower critical end points of the mixtures) are also shown in the same colour convention.

peratures, where the critical points of the two pure components are connected by a continuous critical line; Class 2 includes types III to V where the critical line is not continuous either by divergence of the gas–liquid critical lines or by the interposition of a three-phase line; and type VI (Class 3) where such phenomena as a low-temperature lower critical solution temperature (LCST) along with an upper critical solution temperature (UCST) can form a closed-loop immiscibility window.

Each type will be discussed in section 4 with the help of a suitable example obtained by simulation. Unlike the studies of Scott and van Konynenburg [4], Boshkov and Mazur [6] or Yelash and Kraska [7], to name just a few, the aim of the present work is not an exhaustive study of the complete set of boundaries defining each type of phase behaviour (global phase diagram) for a given equation of state, but rather the illustration of each type of binary mixture using a simple simulation method (the GEMC) and a standard and isotropic intermolecular potential.

3. Computational aspects

As stated in the previous section, all simulations presented in this paper were produced using particles interacting via the one-centre Lennard-Jones (6, 12) potential within the framework of the constant volume GEMC method.

The phase diagrams pertaining to each type of binary mixture were obtained by plotting the corresponding simulation results (pressure, phase density and phase composition at a given temperature, total density and total composition) in the appropriate diagram projection.

Three-box simulations were used whenever three phase equilibria (LLV) were encountered. In regions of the phase diagrams where only two phases were present (LV or LL equilibria), two-box simulations were generally used. In some of these cases three-box simulations were also implemented to check the internal consistency of the results. Single-phase points in the super-critical fluid (SCF) region were also determined with two-box simulations.

All simulation runs were started from partially-filled face-centred cubic lattice configurations with the two components of the mixture placed randomly on the lattice (typically around 600 particles). To avoid biased configurations, the initial volume and numerical density of each box were identical. Ergodicity problems were also avoided starting with boxes of equal composition in cases where liquid–liquid immiscibility was anticipated and with two of the boxes containing two pure samples in cases where total miscibility was expected.

The simulations evolved by the repetitive production of Monte Carlo cycles until equilibration of the system

was achieved and enough configurations were obtained to perform a meaningful statistical treatment (around 50–100 thousand cycles). Each typical cycle consisted of a number of attempted particle displacement moves equal to the number of particles, a number of attempted particle exchange moves equal to half the number of particles times the number of boxes, and a number of volume exchange moves equal to two to ten times the number of boxes. These pre-fixed ratios for each type of move were chosen considering the efficiency with which the simulations attained equilibrium. The fulfilment of the microscopic reversibility conditions at every step of the simulation were guaranteed by the implementation of the same selection algorithms and acceptance criteria used in previous works [3, 8].

The displacement moves were performed by adding a random value from a uniform distribution to the coordinates of the particle undergoing the displacement. The maximum value of the displacement in each box was updated in order to achieve a move acceptance ratio of 50%. The volume exchanges were also randomly chosen from a uniform distribution and the maximum volume exchange was also adjusted to produce an acceptance ratio of 50% for any given pair of boxes. During this type of move the potential energy in each of the boxes affected by the change was calculated using the scaling properties of the Lennard-Jones potential (separation of the repulsive and attractive terms).

Two types of problem had to be accounted for during the simulation runs.

- (i) When the number of boxes exceeds the number of phases or when the size of a given box is small (for instance in conditions close to a dew or bubble point), finite-size effects can be important. To avoid such situations simulation runs were automatically aborted whenever the box size was smaller than a cut-off distance around 3 times the Lennard-Jones interaction diameter, σ . Scaling-up the system or changing its overall composition or density solved this type of problem most of the time.
- (ii) In points close to a critical line or point, for instance near the gas–liquid critical line (LV to SCF transition) or the liquid–liquid critical solution end point (LLV to LV transition), finite-size effects can take the form of identity exchange between the simulation boxes. In these cases the statistical treatment of the simulation results can still be performed using composition and density histograms extended to all boxes. However, with points very close to the critical point/line even this approach will fail. With the present simulation method the position

of a critical point/line has to be inferred from simulations on both sides of the boundary.

The best way to describe a given binary mixture type is to define the relations between the invariant and univariant state points (points and lines) in the corresponding phase diagram. The GEMC technique, either in its original formulation or extended to three-box simulations, can determine by direct simulation state points on the saturation lines of the pure components (LV), on the three-phase line of a partially immiscible liquid mixture (LLV), on the two-phase surfaces of a mixture (LV, LL) or in its single-phase region (SCF). As stated in the previous paragraph, the points corresponding to the end of those lines and the lines bounding the two-phase surfaces have to be inferred by multiple simulations. This implies a large uncertainty in the determination of the locus of those points but phase diagrams belonging to a given type in a clear-cut way will not be ambiguous.

However, special care has to be taken when going from a succession of univariant state points (for example along a three-phase line) to a bivariant region (a two-phase surface). On the line, and as long as the finite size effects pointed above are avoided, the total density and composition can be varied at will since the density and composition of each phase are fixed by the temperature of the system (Gibbs phase rule). On the other hand, on the two-phase surface, these two quantities are no longer determined solely by the system temperature. In order to delimit correctly the critical point it is important that all simulations close to it have the same total composition and number density.

4. Results

4.1. Mixture I

From the conceptual point of view type I mixtures are the most simple: the usual conditions required for a binary mixture to comply with type I behaviour (absence of liquid–liquid immiscibility) are that the characteristics of the two components are alike, i.e. have comparable critical properties and similar intermolecular interactions. A ‘colour’ mixture, where two identical components are differentiated only by an attribute (colour, label) that does not affect in any way their mutual interactions is the textbook example of a type I mixture. More realistically, small departures from this ‘total identity’ still yield mixtures with no liquid–liquid immiscibility zones in the fluid region.

As expected, mixtures of type I were among the first to be studied by GEMC simulation [9], including systems exhibiting azeotropic behaviour and large differences in component size.

Table 1. Interaction parameters for the five mixture types studied.

Mixture type	σ_{11}	σ_{12}	σ_{22}	ε_{11}	ε_{12}	ε_{22}
I	1	1	1	1	1.095	1.2
II	1	1	1	1	0.931	1.2
VI	1	0.85	1	1	0.820	1.2
III	1	1	1	1	1.073	1.8
V	1	0.82	1	1	0.760	1.2

In the present work, mixtures of type I were used to test the validity of the simulation algorithms—comparing two- and three-box simulations with previous 1cLJ simulation results—and to define the basic set of molecular parameters to be used throughout the work. Since the objective of the present paper is to use one binary mixture to illustrate each type of phase behaviour, the working strategy was to concentrate on those sets of parameters that being the most simple would give rise to a clear-cut example of phase behaviour for a given type.

The six Lennard-Jones interaction parameters used for the type I mixture are given in table 1. The two components have equal size and cross-diameter ($\sigma\sigma$) and differ only in their relative volatility (given by different $\varepsilon\varepsilon$). The cross-interaction parameter ε_{12} is given by the geometrical mean of the two pure component parameters (Lorentz–Berthelot rule, LB). The imposed difference in volatility was just large enough so the corresponding p – T phase diagram would have a clear distinction between the two pure component saturation lines.

Simulations were performed at nine different state points and the results are compiled in table 2. Graphs in figures 2(a)–(d) depict the corresponding phase diagram (pressure, composition and density versus temperature and pressure versus composition) projections.

4.2. Mixture II

Type II binary mixtures were considered in a previous article [3] where the GEMC method was extended to a three-box simulation of three coexisting phases (LLV equilibria). In that paper two test cases in binary mixtures were considered where liquid–liquid immiscibility occurred either due to a very unfavourable cross-interaction between the two otherwise similar species—value of ε_{12} smaller than the value given by the LB rule—or due to a large difference between the volatility of the two components. As a matter of fact, the first article applying the GEMC method to mixtures [9] also dealt implicitly with a type II mixture: simulations at relatively high temperatures (not so far removed from the

Table 2. Simulation results for the phase coexistence properties of the five types of mixture studied. X_A is the total mole fraction of component A in the mixture, subscripts I, II and V refer to the two immiscible liquid phases and to the vapour phase, respectively. The number of phases present is also shown.

Mix	X_A	T^*	ϕ	p^*	$x_{A,I}$	$x_{A,II}$	$x_{A,V}$	$d_{A,I}^*$	$d_{A,II}^*$	$d_{A,V}^*$
Type I	0	1.1	2	0.018 (5)	0.000 (-)	-	0.000 (-)	0.745 (20)	-	0.018 (6)
	0.25		2	0.024 (7)	0.241 (9)	-	0.45 (9)	0.728 (18)	-	0.025 (8)
	0.75		2	0.036 (8)	0.742 (16)	-	0.0.86 (7)	0.671 (24)	-	0.045 (12)
	1		2	0.042 (7)	1.000 (-)	-	1.000 (-)	0.643 (24)	-	0.049 (13)
	0.5	2	0.029 (7)	0.490 (12)	-	0.69 (8)	0.702 (18)	-	0.031 (9)	
		2	0.051 (8)	0.486 (13)	-	0.65 (7)	0.648 (25)	-	0.055 (12)	
		2	0.081 (10)	0.483 (17)	-	0.61 (6)	0.575 (26)	-	0.092 (16)	
		2	0.112 (13)	0.488 (12)	-	0.549 (41)	0.488 (31)	-	0.142 (23)	
1		0.152 (20)	0.498 (15)	-	0.507 (41)	0.351 (45)	-	0.295 (48)		
3		0.004 (1)	0.787 (19)	0.136 (5)	0.81 (12)	0.799 (15)	0.838 (14)	0.005 (2)		
3		0.011 (3)	0.607 (8)	0.399 (9)	0.80 (10)	0.755 (22)	0.774 (17)	0.013 (4)		
Type II	0.5	1	2	0.024 (6)	0.482 (14)	0.490 (14)	0.74 (8)	0.715 (20)	0.716 (17)	0.029 (8)
	2	0.044 (8)	0.479 (19)	0.489 (16)	0.69 (7)	0.655 (22)	0.651 (21)	0.052 (13)		
	2	0.079 (10)	0.468 (15)	0.477 (15)	0.640 (44)	0.606 (32)	0.583 (43)	0.107 (25)		
	1	0.169 (21)	0.499 (18)	-	0.502 (20)	0.360 (38)	-	0.336 (35)		
	2	0.007 (2)	0.513 (22)	0.475 (36)	0.88 (13)	1.117 (18)	1.107 (16)	0.010 (3)		
Type VI	0.5	0.8	3	0.016 (4)	0.129 (15)	0.959 (12)	0.82 (14)	0.884 (17)	0.772 (12)	0.020 (5)
	3	0.032 (7)	0.231 (17)	0.921 (21)	0.76 (10)	0.885 (18)	0.735 (14)	0.038 (7)		
	3	0.063 (9)	0.226 (21)	0.846 (22)	0.74 (6)	0.829 (20)	0.690 (22)	0.078 (11)		
	2	0.105 (8)	0.347 (38)	0.407 (44)	0.73 (6)	0.794 (21)	0.792 (22)	0.150 (11)		
	2	0.156 (13)	0.343 (38)	-	0.645 (31)	0.674 (32)	-	0.229 (15)		
	1	0.205 (25)	0.518 (31)	-	0.489 (29)	0.338 (27)	-	0.337 (38)		
	3	0.041 (8)	0.029 (13)	0.956 (16)	0.98 (7)	0.872 (19)	0.645 (18)	0.048 (9)		
Type III	0.5	1.1	3	0.073 (7)	0.051 (14)	0.943 (18)	0.97 (6)	0.845 (21)	0.575 (25)	0.092 (9)
	3	0.090 (10)	0.058 (15)	0.936 (21)	0.96 (6)	0.834 (14)	0.509 (31)	0.116 (10)		
	3	0.127 (11)	0.055 (14)	0.914 (25)	0.935 (41)	0.818 (14)	0.458 (29)	0.224 (15)		
	2	0.233 (32)	0.187 (15)	-	0.891 (31)	0.746 (17)	-	0.266 (35)		
Type V	0.5	0.8	2	0.005 (2)	0.504 (23)	0.486 (24)	0.90 (13)	1.287 (25)	1.294 (19)	0.007 (3)
	2	0.016 (5)	0.491 (25)	0.493 (24)	0.86 (14)	1.211 (23)	1.214 (21)	0.020 (6)		
	2	0.038 (5)	0.484 (20)	0.483 (21)	0.82 (12)	1.117 (29)	1.109 (28)	0.047 (8)		
	3	0.060 (13)	0.248 (21)	0.917 (21)	0.74 (6)	0.882 (20)	0.677 (21)	0.072 (15)		
	3	0.098 (19)	0.247 (27)	0.876 (22)	0.698 (50)	0.830 (19)	0.578 (25)	0.118 (25)		
	2	0.161 (26)	0.260 (26)	0.663 (23)	0.678 (39)	0.765 (18)	0.307 (51)	0.213 (47)		
	2	0.211 (31)	0.288 (22)	-	0.574 (31)	0.650 (23)	-	0.285 (42)		

mixture critical point) showed the presence of an azeotrope in a system with a low value of ε_{12} . Simulations at lower temperatures (and more simulation boxes) would have shown the occurrence of three phases (LLV) at equilibria.

In the present case six state points were obtained by simulation of a type II mixture. The set of molecular parameters used is presented in table 1 and is identical to the set used for the type I mixture except for a 15% lower value of the cross-interaction ε_{12} . Since both components are quite close in terms of volatility the system will exhibit a three-phase line at pressures above both saturation curves of the pure components, which leads to the presence of an azeotrope (the so-called type IIA). Figures 3(a) to (c) delineate the phase diagram for this type of mixture, with the three-phase line nearly super-

imposed on the saturation curve of the most volatile component in figure 3(a).

4.3. Mixture VI

Mixtures of type VI can be discussed at this point since they share more features in common with mixtures of type I and II than those of types III to V, namely a continuous gas-liquid critical line (cf. figure 1). In addition to the UCST present in type II, type VI mixtures have a low-temperature LCST, and can exhibit what is called closed-loop immiscibility.

Due to the presence of such LCST, the set of characteristics necessary for the occurrence of type VI behaviour in a binary mixture has been a controversial issue. Generally type VI behaviour has been associated with complex mixtures, dominated by strong specific

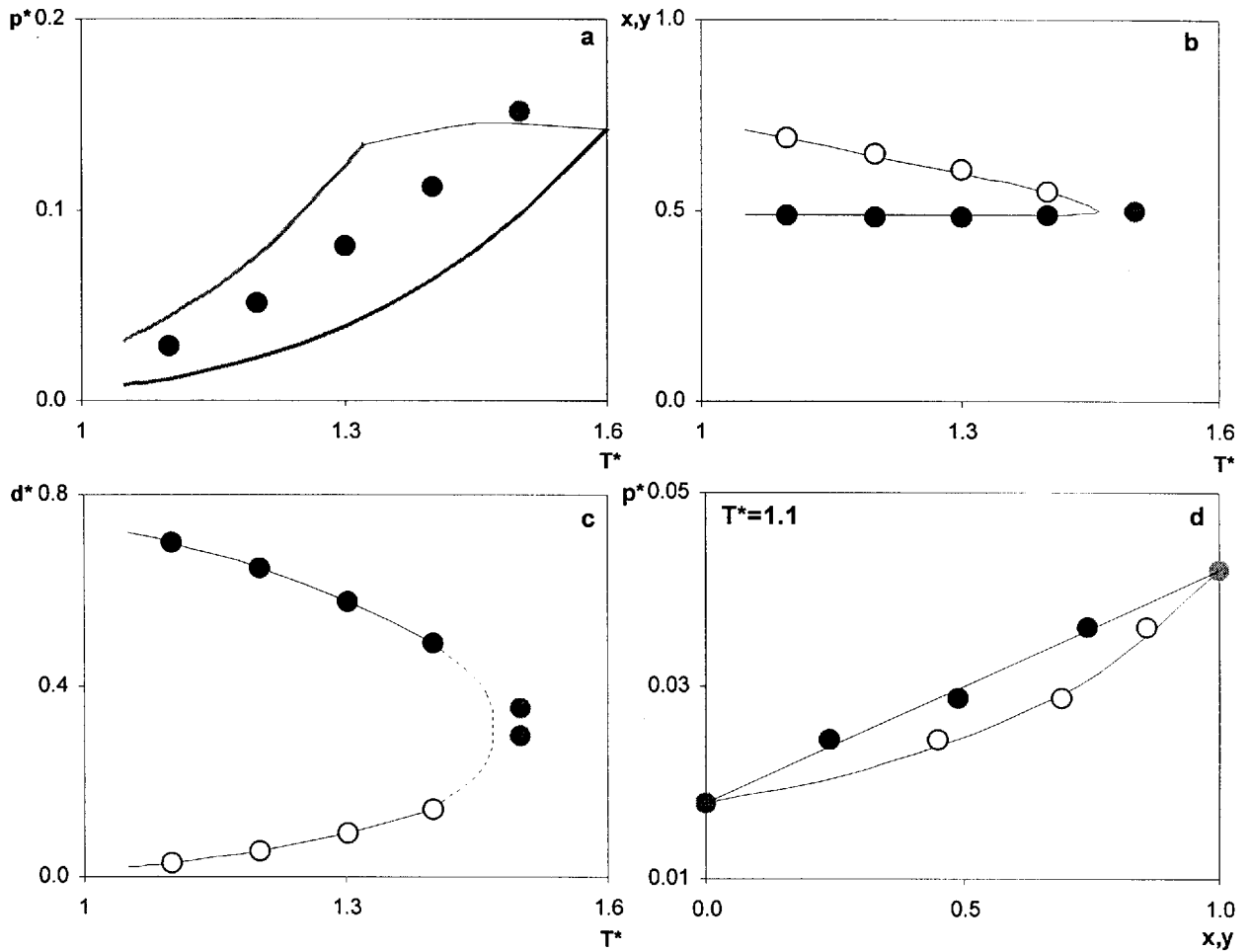


Figure 2. Simulation results for the type I mixture presented as p - T , x - y - T , d - T and p - x - y phase diagram projections. The star superscript denotes the use of reduced units, d is the numerical density of each phase. Each circle represents one state point obtained by simulation. In (a): black circles are in the two-phase region; the grey circle is in the single phase region (supercritical). In (b) and (c): black, empty and grey circles represent liquid, vapour and supercritical fluid properties, respectively. In (d) black, empty and grey stand for liquid, vapour and pure component properties, respectively. The thick grey lines representing the two pure substances were taken from previous 1cLJ simulations [1, 3]. The black lines representing three-phase lines, critical lines, dew and bubble point lines are used just as guidelines to the visualization of the state points.

interactions between the two components (anisotropic attractive forces and/or shape) and several authors stated that closed-loop behaviour is only possible in binary mixtures with cross-association [10] and cannot be represented by a simple ‘one-fluid’ equation of state (EOS) [4]. However, recent work showed that type VI behaviour can be found in isotropic systems using equations of state derived under the one-fluid approximation theory in mixtures interacting via the one-centre Lennard-Jones, 1cLJ, potential [5] or via a hard-sphere with isotropic mean-field attraction, CSvdW, potential [6]. This is specially relevant for the present study since the potential used in all simulations is isotropic (1cLJ).

In order to illustrate a type VI behaviour the molecular parameters were fixed according to the values presented in table 1: the pure component parameters

are still the ones used for the two previous mixtures, the cross-interaction parameter ε_{12} is even less favourable than in mixture II and is responsible for the presence of the UCST, and the cross-interaction diameter σ_{12} is smaller than both the pure component diameters and originates the appearance of the low-temperature LCST (see below). Simulations were performed at seven different state points and the results are shown in table 2. Figures 4(a) to (c) delineate the phase diagram for this type of mixture. Figure 4(a) shows clearly the possibility of closed-loop immiscibility.

The most significant issue in the discussion of this type of mixture is to understand the existence of the LCST, i.e. why two immiscible liquids at moderate temperatures mix into a single liquid phase when the temperature is lowered.

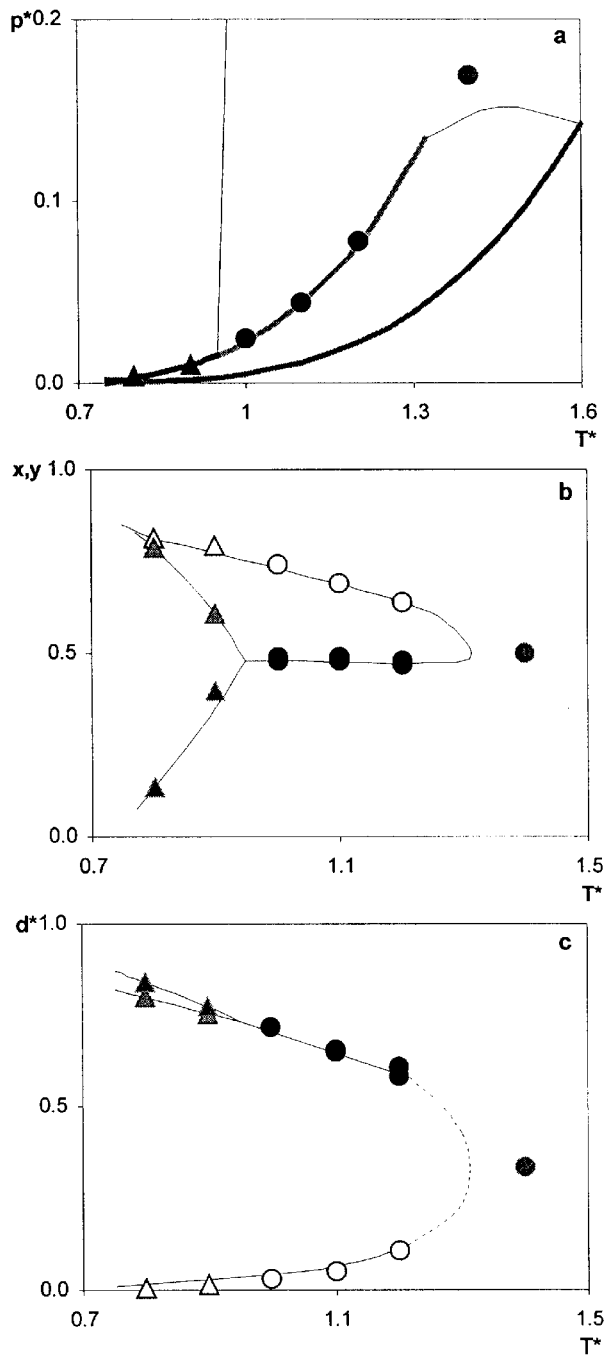


Figure 3. Simulation results for the type II mixture presented as p - T , x - y - T and d - T phase diagram projections. Triangles represent state points on the three phase line. In (b) and (c) light and dark grey triangles represent the two immiscible liquid phases, rich in the more volatile and in the less volatile component, respectively. The other symbols and colours are as in figure 2.

An important fact to be noticed in the simulation results is that the low-temperature single liquid phase forms a non-random mixture between the two components. This can be seen in the pair radial distribution

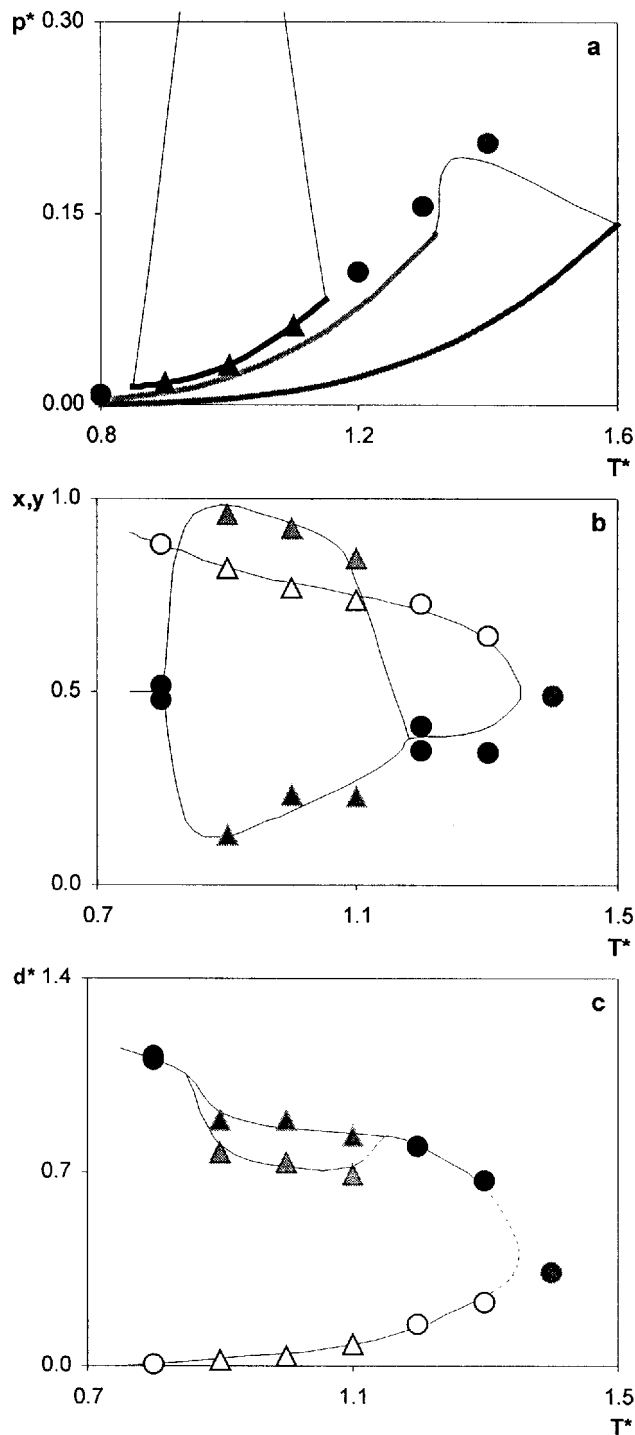


Figure 4. Simulation results for the type VI mixture presented as p - T , x - y - T and d - T phase diagram projections. Symbols and colours as in figure 3.

functions, $g(r)$, shown in figure 5: the heterogeneous pair function shows a first peak at closer distances than the homogeneous pair functions. This feature reflects a sort of cross-association at high liquid densities and is a direct result of the small cross-interaction dia-

meter used in the simulations. This ‘packing’ induced cross-association will also cause the closing of the immiscibility window (closed loop) in the liquid–liquid high pressure/high density region.

Three conclusions can be drawn from the simulation results: first, an isotropic potential can lead to a type VI binary mixture; second, the cross-association found in the low-temperature liquid phase is not incompatible with an isotropic potential and can be originated solely by a small value of the interaction cross-diameter; and finally the closed loop immiscibility can be understood as the result of two opposite trends: cross-association (low σ_{12}) at high liquid densities/low temperatures and an unfavourable cross-interaction (low ϵ_{12}) at moderate densities/temperatures. Both effects decrease with increasing temperature originating the presence of an UCST at higher temperatures. There is no interference of the liquid–liquid immiscibility with the gas–liquid critical line.

This type of approach is different from those adopted by other authors investigating the possibility of closed loop behaviour in isotropic model fluids [4–6]. Most of the work relating a given intermolecular potential/equation of state with fluid phase equilibria behaviour was centred on mixtures of equal sized molecules with a cross-interaction diameter (density dependent parameter) given by the Lorentz–Berthelot combination rule. The present work shows that closed loop immiscibility can be present due to a (cross) size effect between two molecules with similar volatility and an unfavourable cross-interaction. The set of parameters used also

allows the immiscibility window to occur entirely inside the liquid region, avoiding ergodicity problems associated with the simulation of very dense liquid or solid phases.

4.4. Mixture III

A mixture of type III can be imagined as a mixture of type II where the immiscibility between the two components became so pronounced that the locus of the UCST moved to higher temperatures, started to interact with the vapour–liquid critical line and produced its discontinuity.

The set of parameters defining a type III system are presented in table 1 and were obtained by increasing the volatility difference between the two components in the previous mixtures (component 2 was made less volatile by increasing the value of ϵ_{22} from 1.2 to 1.8) and making the cross-interaction parameter 20% lower than the value obtained using the geometrical mean rule. As shown in figure 6(a), the three-phase line is again superimposed with the more volatile component saturation curve and only terminates at a point close to the critical point of that component (the corresponding gas–liquid critical line is frequently quite short in these cases). The gas–liquid critical line starting at the critical point of the less volatile component (not represented) shows a divergent behaviour as can be inferred by the state point at 1.5 reduced temperature, still on the two-phase region (table 2). Figures 6(b) and (c) show composition and density versus temperature projections for this type of mixture.

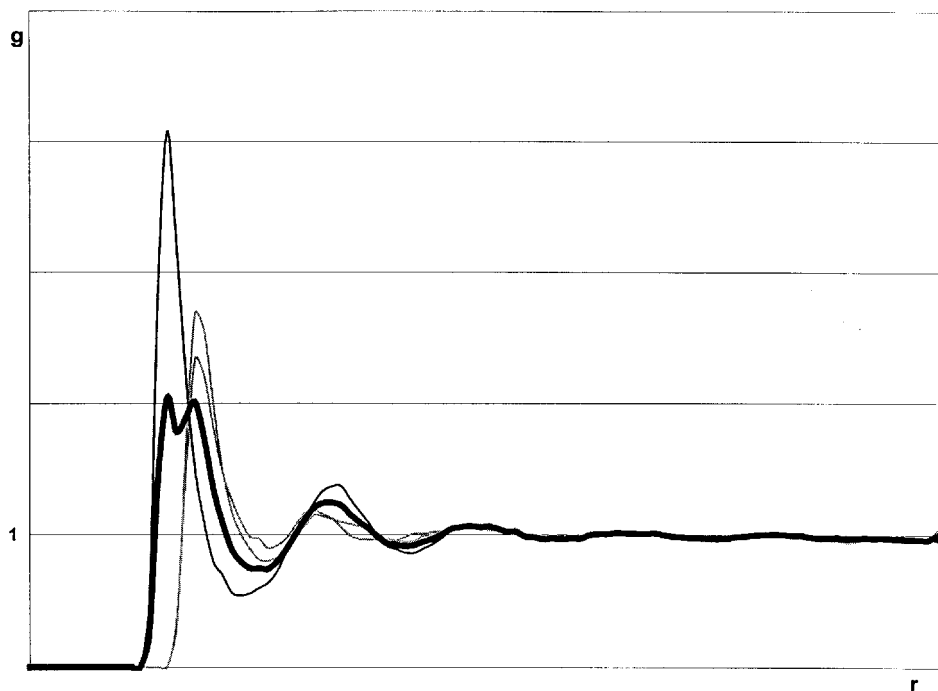


Figure 5. Pair radial distribution function, $g(r)$, of the low-temperature liquid phase of mixture VI. The thin black and grey lines represent the heterogeneous and homogeneous pair distribution functions, respectively; the thick line is the total pair radial distribution function.

4.5. Mixture V

Likewise, mixtures of type V can be regarded as type VI mixtures where the immiscibility window was extended to higher temperatures. In this case not only the UCST point starts to interfere with the liquid–vapour critical line but the two critical lines starting in the LCST and in the critical point of the less volatile component join at higher pressures and densities.

A set of parameters able to describe type V behaviour is presented in table 1 and should be compared with the set corresponding to the type VI mixture: the pure component parameters are the same as in mixtures I, II and VI whereas the cross-interaction parameters are lower than the pure component average. The cross-interaction parameter ε_{12} is even less favourable than in mixture VI, producing an UCST at higher temperatures. The cross-interaction diameter σ_{12} is also lower than in case VI in order to compensate the more unfavourable interaction given by ε_{12} .

Simulation results are presented in table 2 for seven different state points. Figures 7(a) to (c) delineate the phase diagram for mixture V.

Again, the parameters adopted to produce a type V mixture differ from the most commonly used sets of parameters: most authors consider no departures from the Lorentz–Berthelot rule while calculating the cross-interaction diameters. Under such circumstances type V mixtures are found when the two components show large volatility differences and a favourable cross-interaction. Our set of parameters shows that if size effects are taken into account this situation can change dramatically. In fact many real type V mixtures like (methane + 2-methylpentane) show large negative volumes of mixing [11], indicating an effective size effect contribution to the existence of some type V mixtures.

5. Concluding remarks

Binary fluid phase diagrams can be studied using a new version of the Gibbs ensemble Monte Carlo method where three-phase lines are easily defined with the help of three-box simulations.

Critical lines or points cannot be defined precisely with this method (their position has to be inferred by multiple simulations on either side of the critical boundary) and the simulations are limited by the usual constraints of the Gibbs ensemble method, i.e. ergodicity problems start to be important in high-density regions. Nevertheless large areas of the fluid phase diagram can be mapped and the mixture behaviour classified into one of the commonly used types.

As was mentioned before in point 2, this method does not constitute an alternative to the systematic study of phase behaviour that is accomplished by the topological analysis of a given equation of state and the construc-

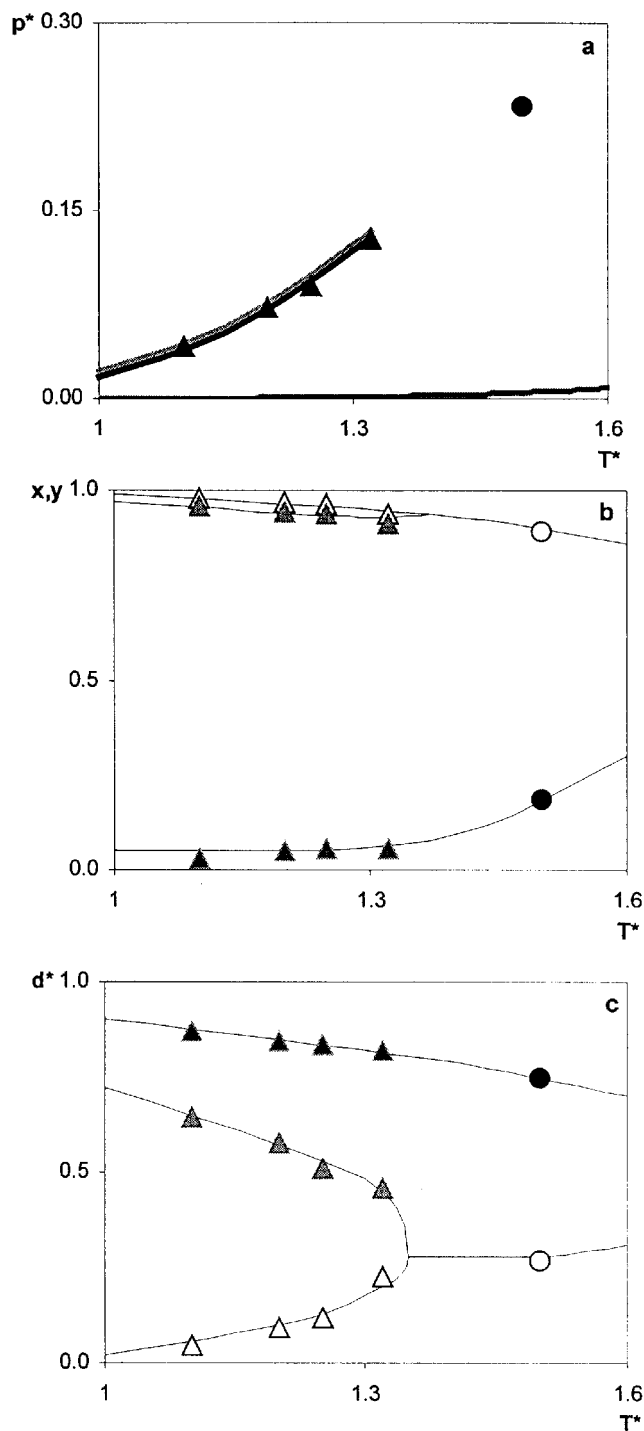


Figure 6. Simulation results for the type III mixture presented as p – T , x – y – T and d – T phase diagram projections. Symbols and colours as in figure 3.

tion of the corresponding global phase diagram. However, it can establish a relation between the simulation results that use directly a given intermolecular potential and the results obtained via the EOS, and therefore can

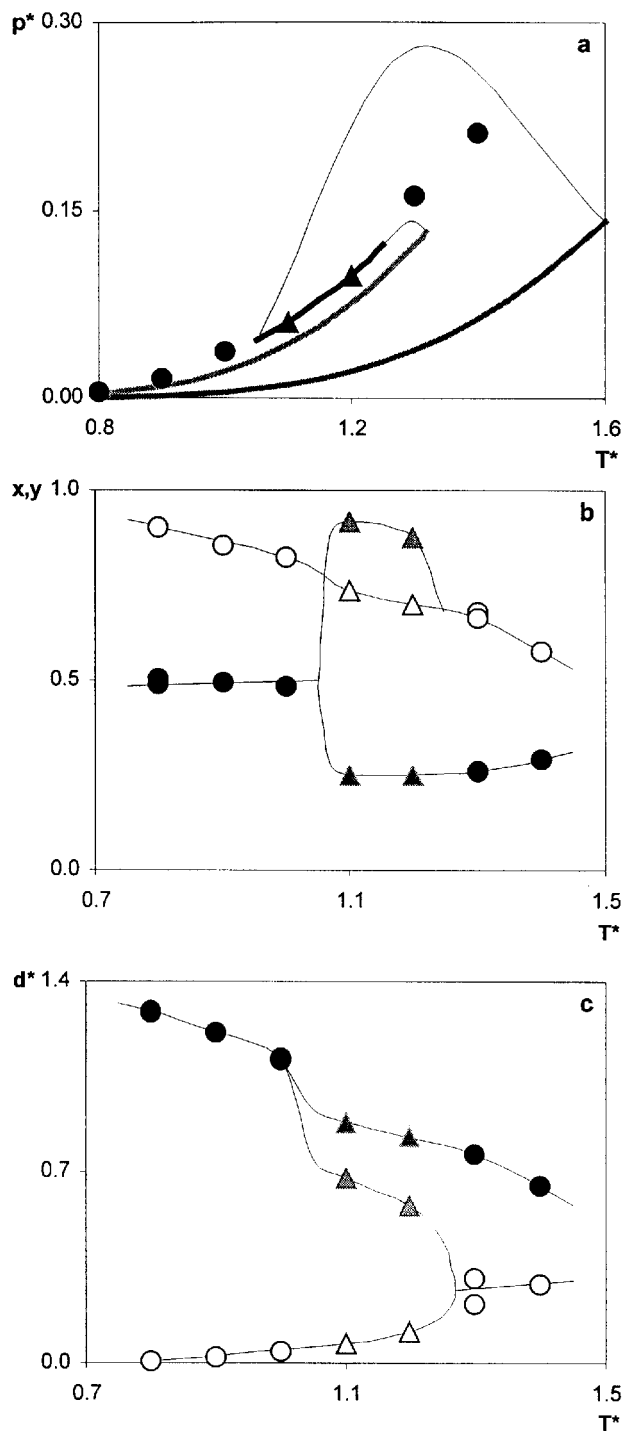


Figure 7. Simulation results for the type V mixture presented as p - T , x - y - T and d - T phase diagram projections. Symbols and colours as in figure 3.

be used to check selected state points in the global phase diagram.

On the experimental side, the simulation of phase diagrams can constitute a direct link between the modelling of a binary mixture and the corresponding fluid phase behaviour. This aspect is specially important since the method is not restricted to any particular kind of potential and can be extended to the study of molecules best represented by other types of intermolecular interaction.

Finally, the versatility of the method was also demonstrated in the simulations of mixtures of type V and VI: departing from the most commonly used sets of parameters it was possible to find for one-centre Lennard-Jones mixtures type V and VI behaviour in uncharted regions of the corresponding global phase diagram.

The author would like to thank J. C. G. Calado for his support and to acknowledge Fundação para a Ciência e Tecnologia (Grant PRAXIS XXI/BPD/6036/95).

References

- [1] PANAGIOTOPOULOS, A. Z., 1987, *Molec. Phys.*, **61**, 813.
- [2] PANAGIOTOPOULOS, A. Z., 1992, *Molec. Simulations*, **9**, 1.
- [3] CANONGIA LOPES, J. N., and TILDESLEY, D. J., 1997, *Molec. Phys.*, **92**, 187.
- [4] VAN KONYNENBURG, R. L., and SCOTT, R. L., 1980, *Phil. Trans.*, **298A**, 495.
- [5] BOSHKOVA, L. Z., 1987, *Dokl. Acad. SSSR*, **294**, 901.
- [6] YELASH, L. V., and KRASKA, T., 1998, *Ber. Bunsenges. Phys. Chem.*, **102**, 213.
- [7] BOSHKOVA, L. Z., and MAZUR, V. A., 1986, *Russ. J. Phys. Chem.*, **60**, 16.
- [8] RULL, L. F., and JACKSON, G., and SMIT, B., 1995, *Molec. Phys.*, **85**, 435.
- [9] PANAGIOTOPOULOS, A. Z., QUIRKE, N., STAPLETON, M., and TILDESLEY, D. J., 1988, *Molec. Phys.*, **63**, 527.
- [10] HILDEBRAND, J. H., 1953, *Discuss. Faraday Soc.*, **85**, 275.
- [11] DAVENPORT, A. J., ROWLINSON, J. S., and SAVILLE, G., 1966, *Trans. Faraday Soc.*, **62**, 322.